Fachtagung "Lasermethoden in der Strömungsmesstechnik"
8.–10. September 2009, Erlangen

Optical Flow and Cross Correlation Techniques for Velocity Field Calculation

Optischer Fluss und Kreuzkorrelation zur Auswertung von Geschwindigkeitsfeldern

R. Kapulla[*], C. Dyck[*], M. Witte[**], J. Fokken[*], A. Leder[**]

[*]Labor für Thermohydraulik (LTH), Paul Scherrer Institut, 5232 Villigen, Schweiz
[**]Fakultät für Maschinenbau und Schiffstechnik, Lehrstuhl Strömungsmechanik, Universität Rostock, 18059 Rostock, Deutschland

Partikelbilder, Optischer Fluss, PIV, Dichtegradient, Mischungsschicht
Particle images, optical flow, PIV, density gradients, mixing layers

Abstract

Calculating velocity fields with the classical cross correlation technique in the presence of strong density gradients faces some unique challenges such as large scale particle image blurring caused by variations of the refractive index in the optical path from the scattering centres to the recording system. The two analysis techniques under consideration are a commercially available standard PIV code and an optical flow based in-house code. The comparison is based on open source test cases (synthetic and real particle images) and PIV images recorded in an isokinetic mixing layer with strong density gradients which deteriorates the image quality in the mixing zone considerably. It is shown that the optical flow method has the potential to compete with PIV when applied to unblurred, 'grainy' Particle images and performs better with partially blurred images; at the expense of computing capacity. However, the underpredicted velocity fluctuations obtained for the optical flow method in the wall boundary layers of the flow, indicate the requirement for further refinement.

1 Introduction

The turbulent mixing of coolant streams of different temperature and density causes severe temperature fluctuations, which may lead to thermal fatigue in the junctions where mixing occurs. Thermal fatigue is a mechanism which results in significant degradation of the mechanical properties of a material exposed to cyclic thermal stresses, which superimposes on the mechanical loads. The aging phenomena resulting from thermal fatigue is the reason for an increased interest in measuring and predicting the flow field and turbulent mixing flow patterns evolving downstream of a mixing point. Due to thermal fatigue, a component may fail before its design lifetime. The water mixing experiments in the GEMIX-Facility – Generic Mixing Experiment, for details see (Fokken et al. 2009) – are focused on the basic mechanisms of turbulent mixing in the presence of density gradients under isokinetic mixing conditions. The two co-flowing streams of the GEMIX facility are initially separated by a splitter plate. In the conditioning section, both streams pass through honeycombs and grids, such that the velocity profiles at the splitter plate tip are flat and free from rotational components. After the tip of the splitter plate both streams interact and form the mixing zone. An open loop water supply driving the test section establishes equal initial velocities for both streams, i.e. isokinetic conditions $u_1 = u_2 = u_0$ in the range from 0.1 to 1 m/s . Additionally, the density ρ of both fluid streams can be adjusted by varying the temperature and adding sucrose to the fluid in one leg to increase the density difference. The GEMIX facility consists of an acrylic glass channel with square cross-section (50×50 mm). The test section is fed from two storage tanks having

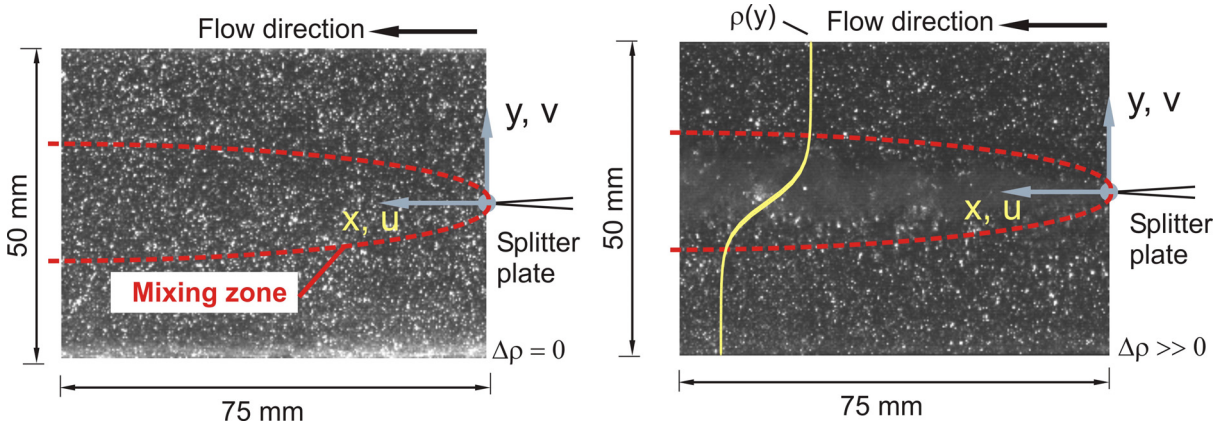

Figure 1: *Particle images recorded close to the splitter plate tip. Without (left) and with strong density gradient (right).*

a volume of 2000 l each. This enables separate conditioning of each stream. The velocity field in the mixing zone was supposed to be studied using Particle Image Velocimetry (PIV). However, calculating velocity fields from particle images in the presence of strong density gradients faces at least a challenge since the variations of the refractive index in the optical path deteriorates the "grainy" particle patterns necessary for the analysis with the standard cross correlation technique. Typical images recorded for the unstratified and stratified conditions are presented in figure 1. These images were recorded in the middle of the channel. For the unstratified case ($\Delta\rho = 0$) one finds a "grainy" particle pattern throughout the whole image plane which allows for the detection of single particles even in the downstream growing mixing zone. In contrast to this, the particle images for the strong stratification ($\Delta\rho \neq 0$) exhibits a strong blurring in the mixing zone, whereas particle images outside this zone remain undisturbed. Applying the standard cross correlation technique to a series of 1024 images without considering the different image characteristics results in a valid vector map as depicted in figure 2. The analysis was performed with the commercial software DaVis 7.2 from LaVision using iteratively decreasing interrogation windows from 64x64 to 16x16. The unstratified case, figure 2 left, shows an almost position independent valid vector occurrence close to 100 % except for the vicinity of the splitter plate tip where it drops down to ≈70 % which is presumably caused by a scale mismatch between the sharp velocity gradient and the spatial resolution of the last interrogation window. In contrast to this, the valid vector occurrence for the stratified case, figure 2 left, can be certainly used to calculate the mixing zone boundaries but the occurrence drop down to values of 75% clearly indicates the limits of the cross correlation technique. Besides the occurrence drop down, we calculated un-physically high standard deviation of velocity in streamwise direction in the mixing zone (not shown here); presumably due to false positive assessed vectors. Introducing optical flow methods for the analysis of partially blurred particle

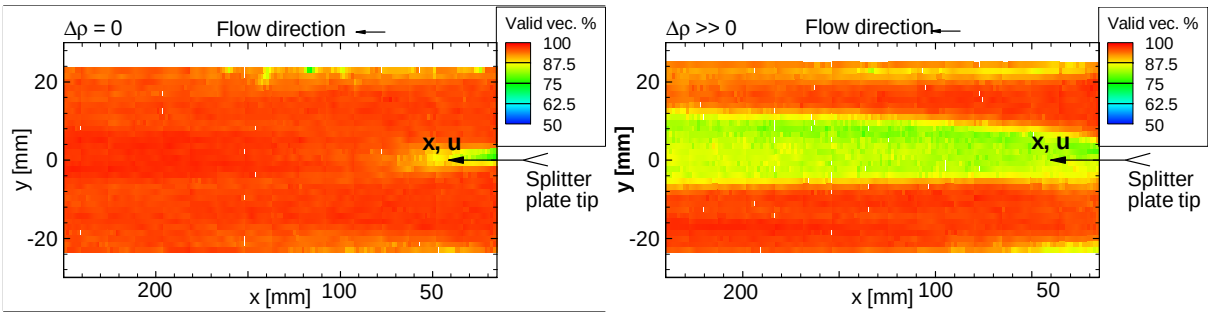

Figure 2: *Valid vector occurence. Without (left) and with strong density gradient (right).*

images to calculate the velocity field might overcome these limitations of the cross correlation method. In the next section we continue with a brief introduction into the optical flow method applied to the images and in continuing sections we compare the cross-correlation and optical flow method for synthetic and experimental images.

2 Theory

The optical flow method implemented for the present experiments is based on the original work of (Horn and Schunk 1981) with the improvements described by (Ruhnau et al. 2005). We will therefore restrict the discussion to basic principles. Optical flow is the distribution of apparent velocities of movement of brightness patterns in an image, according to the definition given in (Horn and Schunk 1981). One can describe the image intensity in an image plane at location (x,y) at time t with I(x,y,t). If the brightness of a particular point remains constant when 'moved' by the local apparent velocity components u=dx/dt and v=dy/dt during a small time instance dt to another location (x+dx,y+dy) between the recording of image pairs, i. e.

$$I(x, y, t) = I(x + dx, y + dy, t + \Delta t) \tag{1}$$

the substantial derivative for the intensity – the brightness transport equation – can be written as:

$$\frac{DI}{Dt} = 0 = \frac{\partial I}{\partial x}\frac{dx}{dt} + \frac{\partial I}{\partial y}\frac{dy}{dt} + \frac{\partial I}{\partial t} = I_x u + I_y v + I_t \tag{2}$$

Since the velocity vector has two components (u,v), whereas the change in brightness at a point provides only one constraint, an additional constraint is necessary to solve Eq. 2. Based on the assumption that neighboring points have similar velocities, a smoothness constraint is introduced by (Horn and Schunk 1981) and (Ruhnau et al. 2005) such that the spatial intensity gradients

$$|\nabla u|^2 = \left(\frac{\partial u}{\partial x}\right)^2 + \left(\frac{\partial u}{\partial y}\right)^2 \text{ and } |\nabla v|^2 = \left(\frac{\partial v}{\partial x}\right)^2 + \left(\frac{\partial v}{\partial y}\right)^2 \tag{3}$$

will be minimized. Since all sort of noise is superimposed to a measurement with real systems, i.e. the intensity remains not exactly constant, but almost constant when moved by the velocity field, the conditions for the velocity field solving Eq. 2, will be relaxed such that the problem posed is to minimize the sum of errors for the brightness transport equation E_B and the departure from smoothness E_C^2, i.e.

$$E_B = \frac{\partial I}{\partial x}\frac{dx}{dt} + \frac{\partial I}{\partial y}\frac{dy}{dt} + \frac{\partial I}{\partial t}$$

$$E_C^2 = |\nabla u|^2 + |\nabla v|^2$$

which results in minimizing the total error E with the weighting factor α^2 – (Horn and Schunk 1981):

$$E = \int\int \{E_B^2 + \alpha^2 E_C^2\} \tag{4}$$

together with finding a suitable velocity field. The discretization of the optimization problem, Eq. 4, is described in (Ruhnau et al. 2005) and is beyond the scope of this article. Since the standard approach introduced by (Horn and Schunk 1981) might cause aliasing if spatial frequencies move more than half of their period between successive frames, a coarse to fine (CTF) velocity field calculation was suggested by (Ruhnau et al. 2005). This is done by calculating a so called Gaussian pyramid. The pyramid is calculated by repeatedly downsampling the image, (Jähne 2005), i.e. for each pyramid level the spatial resolution is reduced by a factor of two. To avoid Moirée-effects (spatial aliasing), a spatial low-pass filter having a cut-off frequency of $\pi/2$ is applied in advance. Suppose we have an image pair (I_0,I_1) with a spatial resolution of 256x256 pixel and we generate 2 pyramid levels. The original image pairs are depicted by upper index L0 (I_0^{L0},I_1^{L0}) and the pyramid levels accordingly as (I_0^{L1},I_1^{L1}) and (I_0^{L2},I_1^{L2}). The image sizes for the Gaussian pyramid amount to L0=256x256, L1=128x128 and L2=64x64, respectively. The initial velocity field estimate $\vec{V}^{L2} = (u^{L2},v^{L2})$ is then calculated

from the coarsest image pair (I_0^{L2},I_1^{L2}) according to the Horn & Schunk algorithm and interpolated onto the next Gaussian pyramid level, i.e. (I_0^{L2},I_1^{L2}) $\rightarrow$ (I_0^{L1},I_1^{L1}) $\rightarrow$ (I_0^{L0},I_1^{L0}). While passing the Gaussian pyramid from coarser to finer levels (L2$\rightarrow$L1$\rightarrow$L0), the intensity patterns from the second image on L2 are shifted (warped, index w) according to the velocity field $\overrightarrow{V}^{L2}$ and a correction-field $\Delta\overrightarrow{V}^{L1}$ is calculated from image pair (I_0^{L1},$I_{1,w}^{L1}$) which adds to the initial velocity estimate, i.e. $\overrightarrow{V}^{L1}=\overrightarrow{V}^{L2}+\Delta\overrightarrow{V}^{L1}$. This correction calculation is repeated until the finest pyramid level is reached. This image warping method is similar to the multi pass approach for standard cross correlation algorithms (Raffel et al. 2007), i.e. an interrogation window shift is applied in a second step according to the velocity calculated in a previous step which increases the correlation strength and therefore, the signal-to-noise ratio. Additional low-pass filtering using again Gaussian filters with cut-off frequencies in the range $[\pi/2, \pi]$ is proposed in (Ruhnau et al. 2005) on each pyramid level before the derivatives are calculated such that the spatial bandwidth is further sliced down. For a given pyramid level this results again in a coarse-to-fine image sequence – the scale levels – for which the velocity estimates are calculated according to the method described above. In contrast to (Ruhnau et al. 2005), the number of scale levels (SL) on each pyramid level is a user parameter for our implementation of the optical flow algorithm. According to (Horn and Schunk 1981) and (Ruhnau et al. 2005), the smoothness parameter (SP) α^2 in Eq. 4 is regarded as a user selectable parameter. Additionally, since the convergence strength of the calculated towards the true velocity field is controlled by α^2 we linearly vary α^2 from high to low values for a given scale level.

3 Code Assessment

The integrity and performance of the optical flow algorithm (OF) implemented was tested with two kinds of particle images documented in the literature and compared with corresponding PIV analysis. For the first kind we used synthetic images from the Visualization Society of Japan (VSJ) where the flow field was calculated using LES. The three synthetic images characterized in (Okamoto et al. 2000) as 2D wall depict a flow region in a downwards projecting jet impinging on a horizontal wall (VSJ 01, VSJ 02 and VSJ 03). These images were also used in (Ruhnau et al. 2005) to asses the code. For the second kind we used real world image which represent the wake vortex forming behind a transport aircraft, (Stanislas et al. 2003), case A. The synthetic images were used to test for the influence of Δt on the result. Images were taken with a Δt of 11, 33, and 99 ms which corresponds to mean particle displacements from 2.5 to 22 pixel. For the PIV analysis we used 2D FFT cross correlation based PIV as implemented in LaVision DaVis V7.2 commercial software. Interrogation window size was reduced from 64$\times$64 to 16$\times$16 with 3 multi-passes and 50 % window overlap. The optical flow calculation for the three synthetic images was performed using 3 pyramid levels, each with 5 scale levels. The smoothness parameter α^2 was adapted along each pyramid level from $\alpha^2/5$ to α^2, and the image low-pass cutoff was varied from $\pi/2$ pixels to π with the final iteration of the calculation being performed on the original image pair. The smoothness parameter was chosen as $\alpha^2 = 0.08/\sqrt{\Delta t}$. The results for OF- and PIV-based results are compared in figure 3. The first column depicts the flow field calculated with the OF method with Δt as parameter. The second column presents the velocity magnitude difference between the OF (subscript OF) and LES (subscript LES) based results. Accordingly, the third and fourth column present the results for the PIV analysis (subscript PIV). Comparing the velocity magnitude difference $|V|_{OF} - |V|_{LES}$ and $|V|_{OF} - |V|_{PIV}$ (column two and four) we find similar error patterns for the OF and PIV results independent of the Δt. For small Δt the magnitude difference $|V|_{OF} - |V|_{LES}$ is close to zero except for the left and lower border where the error increases considerably, figure 3 b) and d). At high Δt both methods break down in the regions of high velocity, figure 3 f) and h). It is good to note, however, that when either method fails to detect the regions of high velocity the rest of the velocity field is not adversely affected. Though a coarse-to-fine velocity field calculation was used, the results are hampered for large Δt by temporal aliasing. In principal the PIV method can detect large particle displacements by using a large initial interrogation window (Raffel et al. 2007), however this can only be extended to the point where out-of-plane

velocities reduces the correlation strength or velocity gradients within the interogation window limit the method.

The results for the vortex image pair can be found in figure 4. The original image was cropped which results in an image size of 512x512. This image pair was characterized as ‘having strong gradients, loss of image density and varying particle image sizes’, (Stanislas et al. 2003). The first row in figure 4 shows the cropped original image pair (left) which experience the already mentioned strong brightness variation between frame #0 and frame #1. To cope with this issue we normalized the brightness, figure 4 right, before applying these images to the OF code. Since no exact solution is available for the case of a real image as is for a synthetic image pair, we compare OF and PIV. The result for u and v components can be found in the middle row of figure 4. Both methods resolve the counter-clockwise rotating vortex with almost the same velocity magnitudes as depicted by the color coding. Extracting the velocities along horizontal and vertical profiles, figure 4 third row, one finds an excellent agreement between OF and PIV such that the profiles collapse identical on each other, except for velocity u calculated with OF which partially fails in the vortex core, figure 4 mark A and B and deviates considerably from the PIV result. Since there is no obvious reason for this deviation additional refined analysis calculations with OF are necessary.

4 Real World Images

The results of both OF and PIV methods are applied to experimental images where stratification in the mixing zone caused strong blurring of the particle images, see figure 1. The measurement plane was located in the middle of the channel. For both OF and PIV 10 images each having a size of 1000x200 pixel were analyzed. The mean (u and v) and standard de-

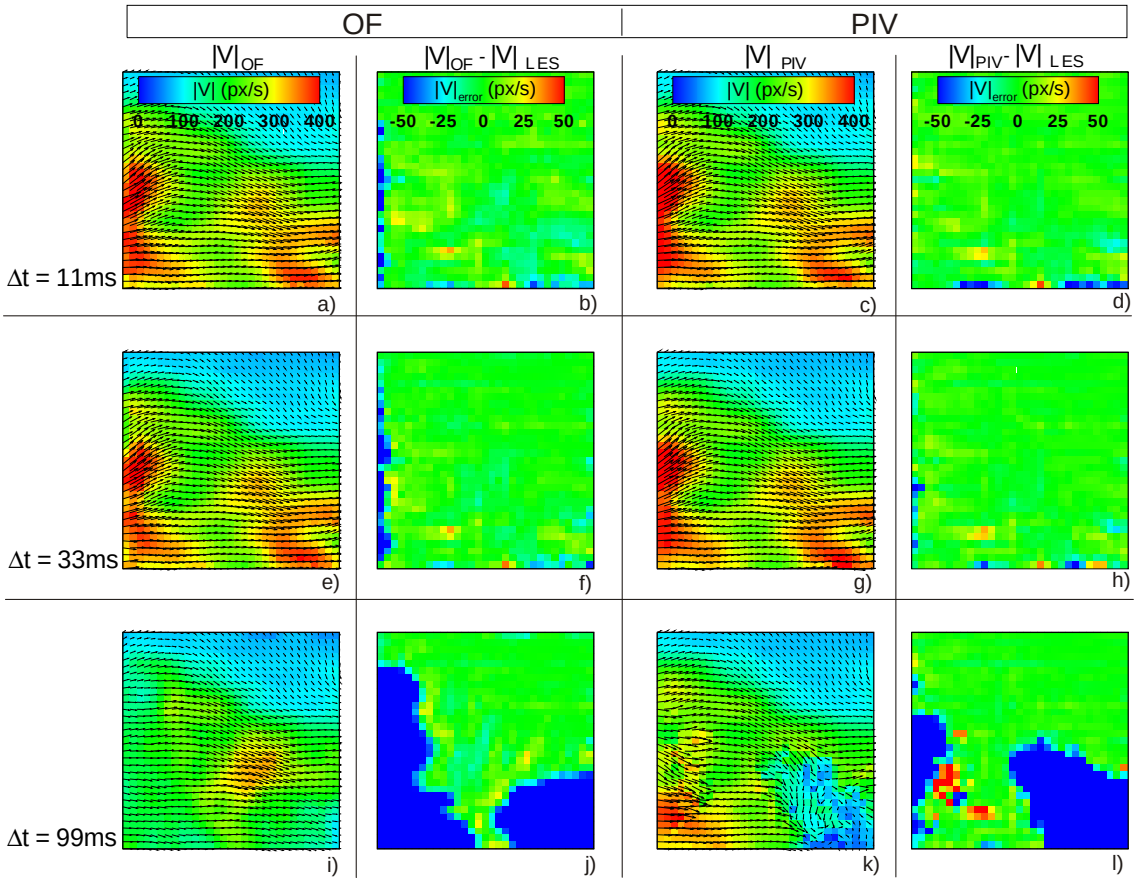

Figure 3: *Comparison of OF-based (left) and PIV based (right) velocity field calculations with LES results. VSJ standard images 01, 02, 03.*

viation (u_{rms} and v_{rms}) in the results from OF (left) and PIV analysis techniques (right) can be found in figure 5. Isokinetic flow velocity is u_0=0.4 m/s from right to left. Velocity profiles were extracted for x=200 mm, figure 6. The comparison of the average streamwise velocity fields (u) for OF and PIV analysis methods shows that the OF technique finds a much smoother field – especially in the mixing zone where the particle images were blurred, figure 5 a) and b). From the same images it is also apparent that OF finds slightly smaller velocities in the main flow streams (y=-10 and y=10 mm) where the original particle images were not distorted. The advantages of the OF method become apparent when comparing the vertical velocity component v, figure 5 b). While OF finds a vertical velocity field which stays very close to zero – in accordance with the expectations – the PIV method introduces a lot of 'noise' in the mixing zone (around y=0 mm), even when the velocity is averaged over 10 images. These false vectors introduced by PIV in the mixing zone also show up in u_{rms} and v_{rms}, figure 5 b) and c). The OF method finds very little variation in either of u_{rms} and v_{rms} throughout the entire measurement plane. However, in the free stream outside the mixing zone (y≈-12 and y≈12 mm) where the particles images are not blurred, the RMS-magnitude is the same for both OF and PIV. The profiles of the mean velocities u and v as well as u_{rms} and v_{rms} were extracted from figure 5 at x=200 mm (dashed line) and displayed in figure 6. A third result was added which was obtained for $\Delta\rho = 0$, i.e. no density stratification and, consequently, no image blurring was present. This reference case was calculated using PIV over a series of 1024 images and is expected to have similar velocity properties as the strong stratified case under examination, except in the mixing zone, where the stable stratification is expected to damp the velocity fluctuations. From figure 6 it is apparent that velocity resulting from PIV analysis is much noisier than that produced by the OF method. Only averaging 10 samples ($\Delta\rho \gg 0$) does not produce a smooth enough result to reliably compare either u or v velocities. The OF method however,

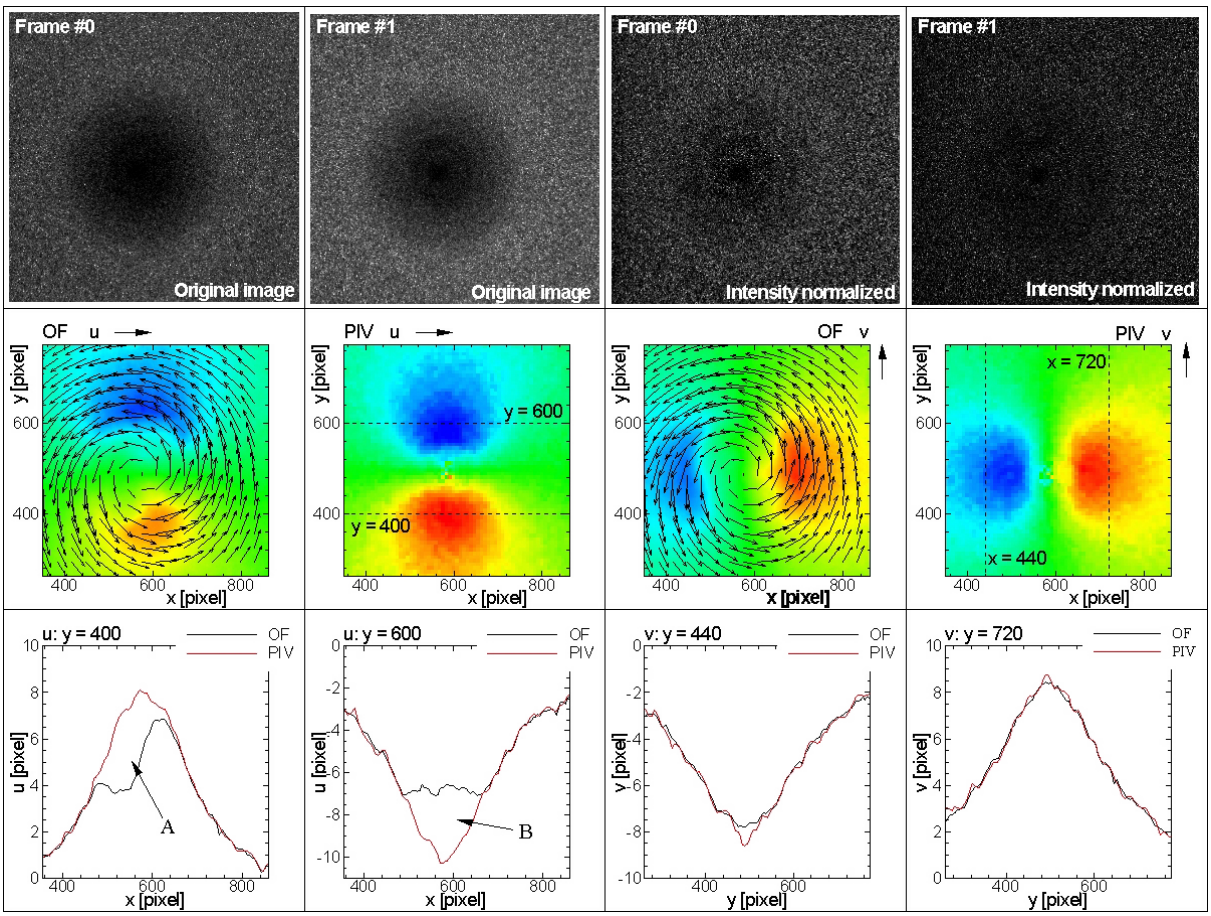

Figure 4: *Comparison of OF-based and PIV based velocity field calculated for the vortex flow.*

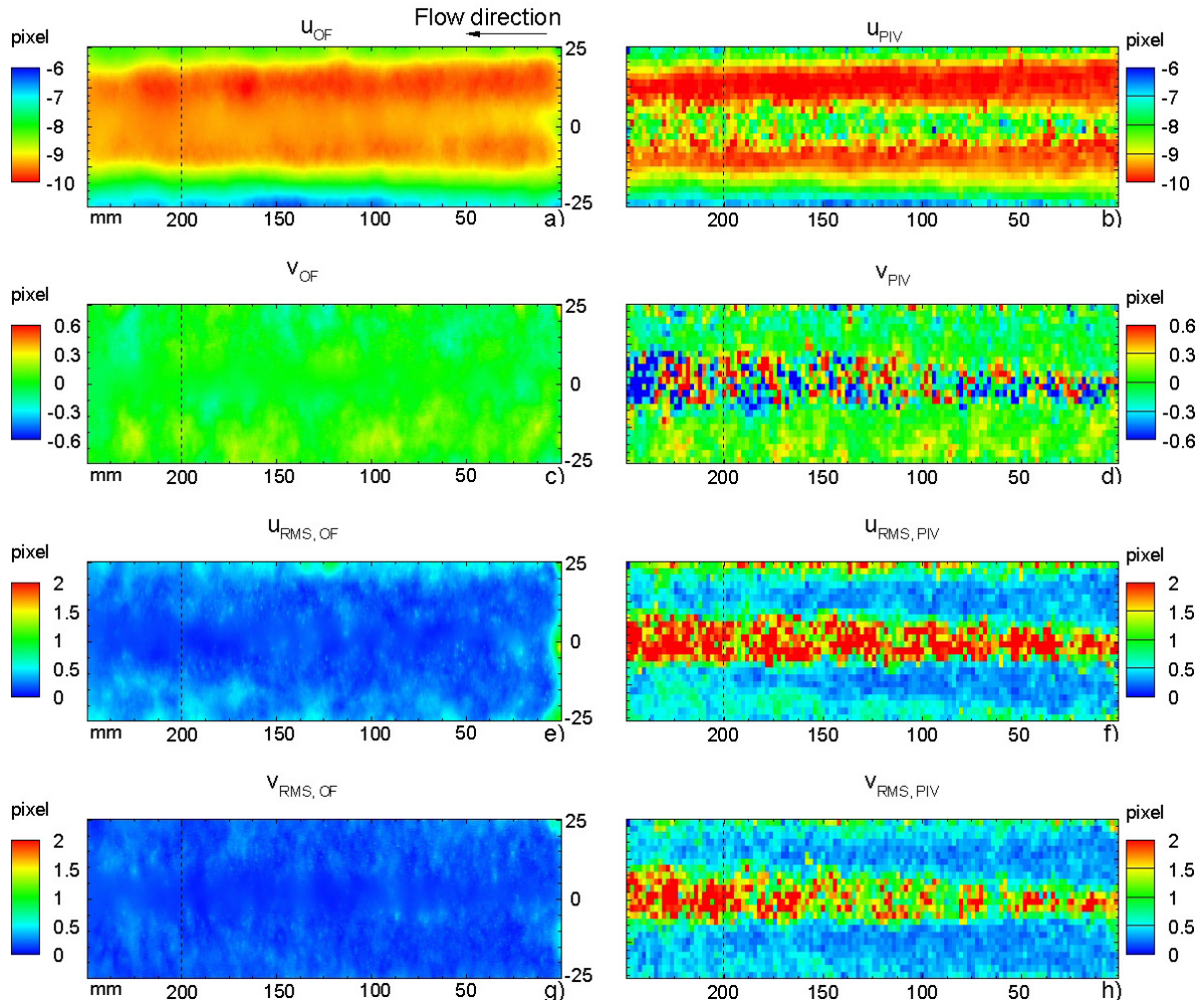

Figure 5: *Velocity field quantities calculated from particle images recorded in a mixing layer with strong density gradient. Statistics are based on 10 images. OF-based (left) and PIV-based results (right).*

produces a result which is almost as smooth after averaging only 10 samples, as the reference case is ($\Delta\rho = 0$) where 1024 samples were averaged. It was shown, however, that the OF method has underestimated both the peak (slightly) of the velocity in the main flow outside the mixing zone, and the magnitude of the velocity deficit, figure 6 c) mark A. Whether the choice

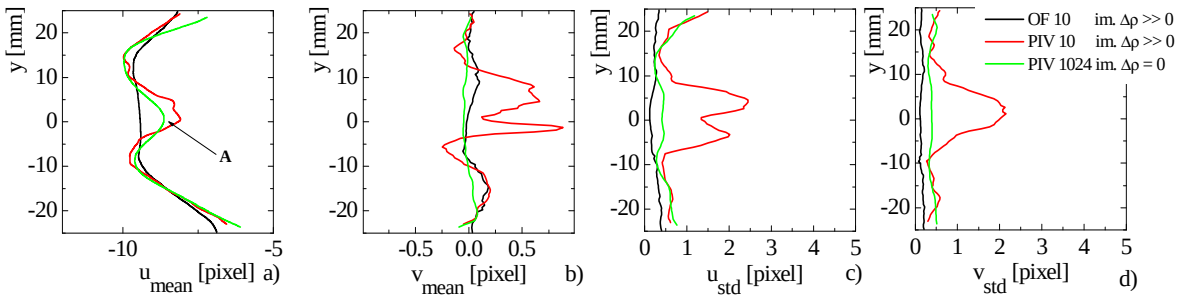

Figure 6: *Velocity field quantities for strong density gradients ($\Delta\rho >> 0$) extracted at x=200 mm from figure 5. Statistics are based on 10 images. For comparison purposes we have added corresponding profiles for ($\Delta\rho = 0$) calculated with PIV.*

of a lower smoothness parameter α^2 could improve the performance of the OF method in this regard, or whether the corresponding increase in sensitivity to image noise at lower α^2 would ruin the OF result is subject to further analysis runs and the application of the OF method to $\Delta\rho = 0$ cases. On the other hand, because the $\Delta\rho \gg 0$ case under consideration has a strong stratification in the mixing zone it is expected that u_{rms} and v_{rms} would be reduced relative to the $\Delta\rho = 0$ case. The PIV results, figure 6 c) and d) $\Delta\rho \gg 0$, contradict this, which is just more proof that the cross correlation method is unable to find correct vectors in the blurred area of the image. The OF results, however, are in line with this assumption. This topic will be subject to further discussions when comparing the experimental with numerical results for $\Delta\rho \gg 0$, see also (Fokken et al. 2009). In the boundary layers growing with downstream distance at the lower and upper part of the test section, figure 6 c) and d) $\Delta\rho \gg 0$, the OF method finds a lower velocity standard deviation than is present for the PIV analysis for either $\Delta\rho \gg 0$ or $\Delta\rho = 0$, which yet is another indication that the OF method requires further refinement, and that a larger sample size is required for a better statistical comparison.

5 Summary and Outlook

An optical flow (OF) technique was applied to calculate the velocity field from partially blurred particle images recorded in a density stratified, isokinetic mixing layer. The integrity and performance of the OF code was successfully tested with synthetic and experimental standard images found in literature. It was shown that the method can compete with the standard cross-correlation PIV approach, and, for strong density gradients, outperforms it in the mixing zone. However, in the wall boundary layers – undisturbed from density gradients – the OF method finds a lower u_{rms} and v_{rms} than is present for the PIV analysis which indicates that the OF method requires further refinement. Whether the choice of a lower smoothness parameter α^2 for OF could improve the performance of the method in this regard, or whether the corresponding increase in sensitivity to image noise ruin the OF result is subject to further analysis and the application to $\Delta\rho = 0$ cases. On the other hand, in the presence of strong density gradients, the OF method results in lower velocity fluctuations in the mixing zone when compared with PIV. This is subject to a comparison with LES calculations.

6 References

Fokken, J., Kapulla, R., Kuhn, S., Dyck, C. and Prasser, H. M. (2009), Stably stratified isokinetic turbulent mixing layers: Comparison of PIV-measurements and numerical calculations, Fachtagung “Lasermethoden in der Strömungsmesstechnik”, 8.–10. September 2009, Erlangen.

Horn, B.K.P and Schunk, B.G.: Determining optical flow. Artificial Intelligence, 17, pp. 185-204, 1981.

Jähne, B. (2005), Digitale Image Processing, 6th revised and extended edition, Springer Verlag.

Okamoto, K., Nishio, S., Saga, T. and Kobayashi, T. (2000), Standard images for particle-image velocimetry, Meas. Sci. Technol., 11, 685-691.

Raffel, M., Willert, C.E., Wereley, S.T. and Kompenhans, J. (2007), Particle Image Velocimetry, A Practical Guide, 2nd ed., Springer Verlag.

Ruhnau, P., Kohlberger, T., Nobach, H. and Schnörr, C. (2005), Variational Optical Flow Estimation for Particle Image Velocimetry, Experiments in Fluids, 38:21-32.

Stanislas, M., Okamoto and Kähler, M. (2003), Main results of the first international PIV challenge, Meas. Sci. Technol., 14:R63-R89.